Cell, Vol. 87, 721–732, November 15, 1996, Copyright ©1996 by Cell Press

Oligomeric Rings of the Sec61p Complex Induced by Ligands Required for Protein Translocation

Dorit Hanein,* Kent E. S. Matlack,† Berit Jungnickel,† Kathrin Plath,†‡ Kai-Uwe Kalies,‡ Kenneth R. Miller,§ Tom A. Rapoport,† and Christopher W. Akey*
*Department of Biophysics
Boston University School of Medicine
Boston, Massashusetts 02218-2394
†Department of Cell Biology
Harvard Medical School
Boston, Massachusetts 02115
‡Max Delbrueck Center for Molecular Medicine
Robert Roessle Str. 10
13122 Berlin-Buch
Germany
§Division of Biology and Medicine
Brown University
Providence, Rhode Island 02912

Summary

The heterotrimeric Sec61p complex is a major component of the protein-conducting channel of the endoplasmic reticulum (ER) membrane, associating with either ribosomes or the Sec62/63 complex to perform co- and posttranslational transport, respectively. We show by electron microscopy that purified mammalian and yeast Sec61p complexes in detergent form cylindrical oligomers with a diameter of ~85 Å and a central pore of ~20 Å. Each oligomer contains 3–4 heterotrimers. Similar ring structures are seen in reconstituted proteoliposomes and native membranes. Oligomer formation by the reconstituted Sec61p complex is stimulated by its association with ribosomes or the Sec62/63p complex. We propose that these cylindrical oligomers represent protein-conducting channels of the ER, formed by ligands specific for co- and posttranslational transport.

Introduction

Protein transport across the membrane of the ER can be either co- or posttranslational in all organisms (for review, see Walter and Johnson, 1994; Rapoport et al., 1996). In the cotranslational pathway, which predominates in mammalian cells, the nascent polypeptide chain is transferred across the membrane concomitant with its synthesis on a membrane-bound ribosome. In the posttranslational pathway, used extensively in yeast, the ribosome plays no role, and the polypeptide can be transported through the membrane even after completion of translation. It is believed that transport occurs through a protein-conducting membrane channel in both pathways. For the cotranslational pathway, it has been hypothesized that the channel is formed de novo for each translocation event (Blobel and Dobberstein, 1975). Hence, upon arriving at the membrane, the ribosome-nascent chain complex would trigger channel formation by inducing the lateral association of transmembrane proteins and would stabilize their association by direct contact throughout translocation (Blobel and Dobberstein, 1975). How similar channels would form in the posttranslational pathway is unclear. Other models have made more specific predictions about the channel, postulating 3–6 related but nonidentical subunits (Singer et al., 1987), an amphiphilic interior (Rapoport, 1985), and lateral gating to allow hydrophobic segments of membrane proteins to exit into the surrounding lipid bilayer (Singer et al., 1987; Simon and Blobel, 1991).

The existence of a channel is supported by two types of experiments. Electrophysiological measurements on membranes performing cotranslational translocation demonstrated that large ion-conducting channels appear when nascent chains are released from membrane-bound ribosomes by puromycin (Simon and Blobel, 1991), consistent with the translocating chains occupying transmembrane channels prior to their release. Experiments in which fluorescent probes were incorporated into the nascent chain showed that they cross the membrane in a hydrophilic environment, supporting the idea of passage through an aqueous channel (Crowley et al., 1993, 1994). The latter experiments confirmed that the nascent chain is transferred directly from the ribosome into a tightly associated membrane channel. Further experiments demonstrated that the channel opens toward the lumen only after the growing nascent polypeptide chain has reached a certain length (Crowley et al., 1994), probably due to an interaction between the signal sequence and a membrane component (Jungnickel and Rapoport, 1995), which may be a constituent of the channel. Despite these insights into the function of the ER channel, its structure and mechanism of formation are unknown.

Complementary approaches, including genetic screens in yeast and biochemical experiments in yeast and mammals, have led to the identification of the heterotrimeric Sec61p complex as the major component of the protein-conducting channel of the ER (Deshaies and Schekman, 1987; Rothblatt et al., 1989; Görlich et al., 1992; Panzner et al., 1995). The Sec61p complex is highly conserved (Görlich et al., 1992; Hartmann et al., 1994), with subunits of the mammalian complex (Sec61α, Sec61β, and Sec61γ) being similar in sequence to those in S. cerevisiae (Sec61p, Sbh1p, and Sss1p) (Panzner et al., 1995). Genetic studies and biochemical reconstitution experiments indicate that the Sec61p complex is an essential translocation component (Deshaies and Schekman, 1987; Rothblatt et al., 1989; Görlich and Rapoport, 1993). Cross-linking experiments have demonstrated that the largest subunit of the complex (Sec61α or Sec61p), with 10 membrane-spanning domains, is in close proximity to a polypeptide chain as it passes through the membrane (Kellaris et al., 1991; Görlich et al., 1992; Müsch et al., 1992; Sanders et al., 1992; High et al., 1993; Nicchitta et al., 1995; Do et al., 1996). Experiments in the mammalian system showed that as the translocating nascent chain crosses the phospholipid bilayer, every amino acid of the segment within the plane of the membrane can be cross-linked to Sec61α (Mothes et al., 1994); no other membrane

protein gives strong cross-links to any of those residues, suggesting that Sec61α surrounds the nascent chain continuously from one side of the membrane to the other.

The cotranslational mode of protein transport across the mammalian ER membrane can be reproduced with proteoliposomes reconstituted from three purified membrane protein components (Görlich and Rapoport, 1993): the signal recognition protein receptor, the Sec61p complex, and the translocating chain–associating membrane protein. Under certain conditions, the Sec61p complex alone in the phospholipid bilayer suffices for translocation (Jungnickel and Rapoport, 1995). In promoting translocation, the Sec61p complex anchors the ribosome to the membrane and is required for a signal sequence recognition event within the membrane (Kalies et al., 1994; Jungnickel and Rapoport, 1995). In the cotranslational pathway of yeast, the heterotrimeric Sec61p complex may function in a similar manner.

The Sec61p complex is also likely to form the core of the posttranslational translocation machinery. Posttranslational protein transport in yeast can be reproduced with reconstituted proteoliposomes that contain a heptameric membrane protein complex consisting of the trimeric Sec61p complex and the tetrameric Sec62/Sec63p complex (Sec62p, Sec63p, Sec71p, and Sec72p) (Panzner et al., 1995). Neither of the subcomplexes supports posttranslational translocation when reconstituted separately, but activity is restored to the original level if they are recombined during reconstitution. Taken together, the present evidence makes the Sec61p complex a compelling candidate to form the protein-conducting channel in both translocation pathways. How the Sec61p complex forms an active channel and the possible role of the ribosome or the Sec62/63p complex in channel formation or gating are unknown.

We now report that the Sec61p complex forms cylindrical oligomers with a central pore when isolated in detergent and when present in membranes. In membranes, formation of cylindrical oligomers is greatly stimulated by direct interaction of the Sec61p complex with either ribosomes or the Sec62/63p complex, ligands required for co- and posttranslational translocation, respectively. We propose that these oligomeric assemblies of the Sec61p complex represent the elusive protein-conducting channels of the ER.

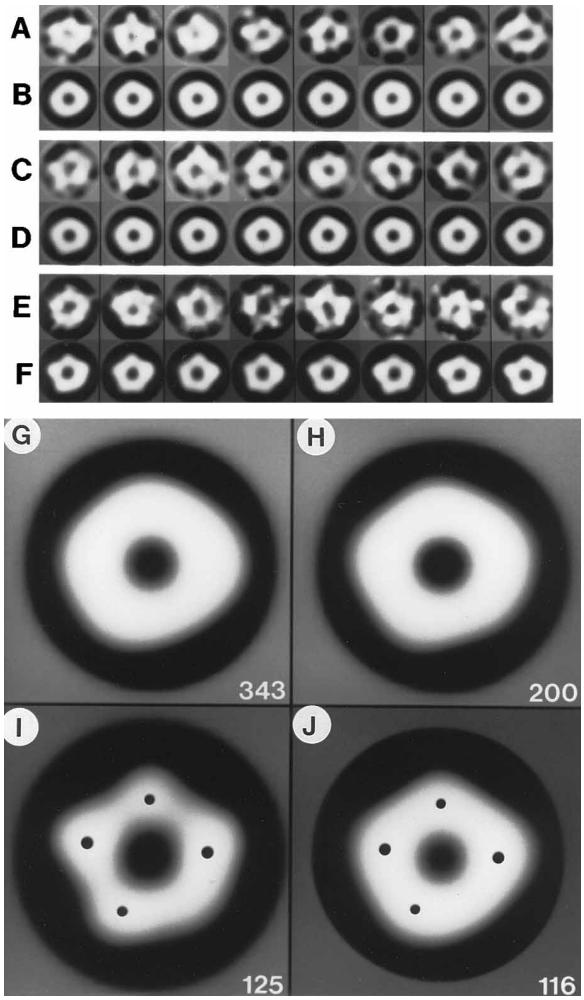

Figure 1. Individual Images and Averaged Projection Maps of the Sec61p Complex

(A) Individual particles of the canine Sec61p complex viewed in negative stain.

(B) Averaged maps obtained using the corresponding single molecules of (A) as references.

(C and D) Individual yeast Sec61p complexes and corresponding averages viewed in negative stain.

(E and F) Individual frozen-hydrated particles of the canine Sec61p complex and corresponding averages.

(G) Global average of all particles of canine Sec61p complex in negative stain (diameter of 83 Å with a central pore of 19 Å).

(H) Global average of all particles of yeast Sec61p complex in negative stain (diameter of 82 Å with a central pore of 21 Å).

(I) Global average of all particles of canine Sec61p complex in ice (diameter of 90 Å with a central pore of 23 Å).

(J) A selected map obtained from classification analysis of the combined canine/yeast data sets in negative stain. The positions of consistent density peaks are shown with dark dots in (I) and (J). The number of particles analyzed is shown in the lower right-hand corner of (G)–(J).

Results

Morphology of the Purified Sec61p Complex in Detergent

We first used electron microscopy to study purified, detergent-solubilized Sec61p heterotrimers from mammals and yeast. Dog pancreatic Sec61p complex was purified from detergent-solubilized RM using the ribosome-associated fraction as starting material (Görlich and Rapoport, 1993). The equivalent complex from S. cerevisiae was purified from the nonribosome-associated fraction of membrane proteins by ion-exchange chromatography (Panzner et al., 1995).

In negative-stain electron microscopy, the mammalian and yeast complexes have the appearance of rings with a central stain-filled pore (Figures 1A–1D and 2A). The majority of the particles have approximately the same diameter and a quasipentagonal shape in projection. However, smaller particles of a different morphology were present in variable amounts. For single-particle image analysis, we scanned ~60 micrographs and

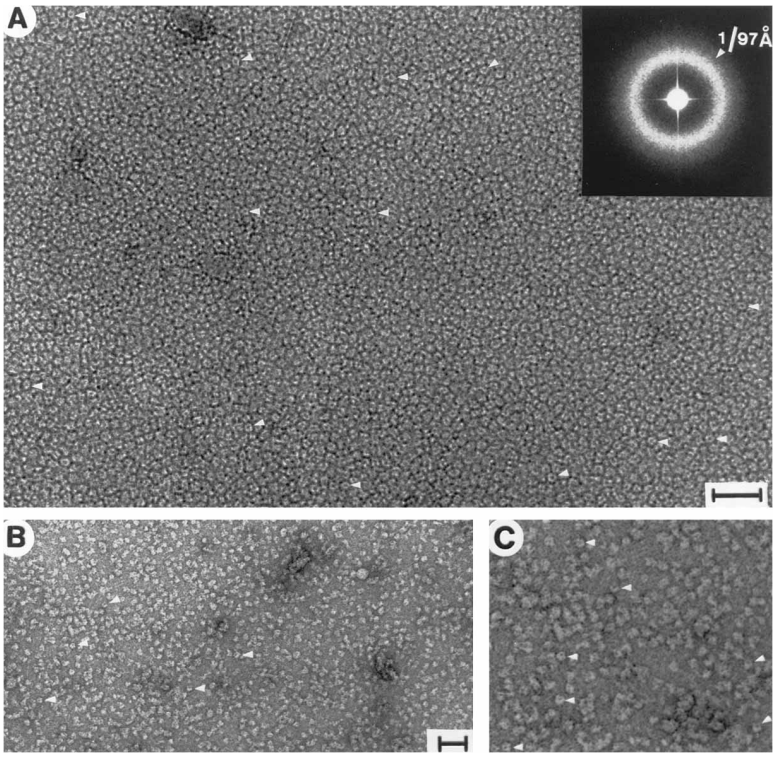

Figure 2. Negatively Stained Translocation Complexes

(A) The trimeric canine Sec61p complex in a close-packed array. Particular examples of ring-like structures are indicated by arrowheads. Smaller molecular fragments can be seen between the rings. Inset: summed powder diffraction pattern from $\sim 2.5 \times 10^5$ oligomers, with a first order spacing of 1/97.5 Å. Scale bar = 500 Å.

(B) The heptameric Sec complex from S. cerevisiae at low magnification (scale bar = 500 Å). Most particles are globular and do not show a ring morphology.

(C) The Sec complex at higher magnification, scale as in (A): asymmetric complexes with stain-filled pores that are generally located off center (see arrowheads).

chose the best face-on particles based on size and the presence of a central pore (n = 543). To minimize subjectivity in the analysis, we used a combination of reference-dependent and multireference alignment strategies in the averaging. Figures 1A and 1C show selected reference particles for the negatively stained dog and yeast Sec61p complexes, respectively. Figures 1B and 1D show the corresponding averages after alignment of each reference particle with the total canine and yeast particle populations, respectively. The individual averages are strikingly similar for the complexes from the two organisms, with both data sets showing a quasipentagonal geometry. Global multireference averages were calculated from the individual averages (9 for the dog and 12 for the yeast Sec61p complexes) and are shown as grayscale maps in Figures 1G and 1H. These averages confirm the rounded quasipentagonal morphology of the Sec61p complexes in detergent. Upon classification of the combined data from both species, in several classes (one of which is shown in Figure 1J), the quasipentagonal structure was obvious. The molecules have an average diameter of ~85 Å with a central pore of ~20 Å diameter.

An independent estimate of the upper size limit was obtained by negative-stain electron microscopy for the dog pancreatic Sec61p complex, using conditions where the particles form a close-packed monolayer on the grid (see Figure 2A). An average interparticle distance of 97 Å was calculated from the first order powder diffraction ring calculated from images containing $\sim 2.5 \times 10^5$ molecules (see the inset in Figure 2A). This value represents an upper estimate of the particle diameter, since a fraction of smaller molecules is interdigitated among them, thereby enlarging the true spacing.

To rule out the possibility that the observed oligomeric structure of the Sec61p complex, and in particular its central pore, is an artifact of negative staining, we analyzed rapidly frozen, unstained specimens of the dog pancreatic complex by electron microscopy. The unstained particles had very similar morphologies to those seen in negative stain, except that the quasipentagonal geometry was more pronounced (individual particles and their alignment averages are shown in Figures 1E and 1F, and the overall average is in Figure 1I). The particles were somewhat larger in diameter, possibly due to differences in bound detergent and problems associated with determining the edge of the particles. Also, the pore appears larger in the map of the unstained particles, and the density peaks are more distinct, most likely due to a combination of improved preservation of the structure and the loss of very low resolution frequencies in the contrast transfer function, which may enhance features such as the pore and substructure within the ring. Although best seen with the unstained specimens, we consistently observed four density peaks within the ring structure, with two pronounced peaks at 3 and 9 o'clock in the averages, aligned as in Figures 1I and 1J, and less dense features at 12 and 7 o'clock (see black dots in Figures 1I and 1J).

The mammalian and yeast Sec61p rings display a considerable degree of structural polymorphism, as demonstrated by classification analysis of negatively stained data sets (not shown; see Experimental Procedures). Two prominent image variations were found: differences in the diameter of the oligomers (~5% corresponding to 4.3 Å), and parallel, but larger changes in the diameter of the central pores (~40% corresponding to 7 Å; i.e., pores range from 16–23 Å). Such variations

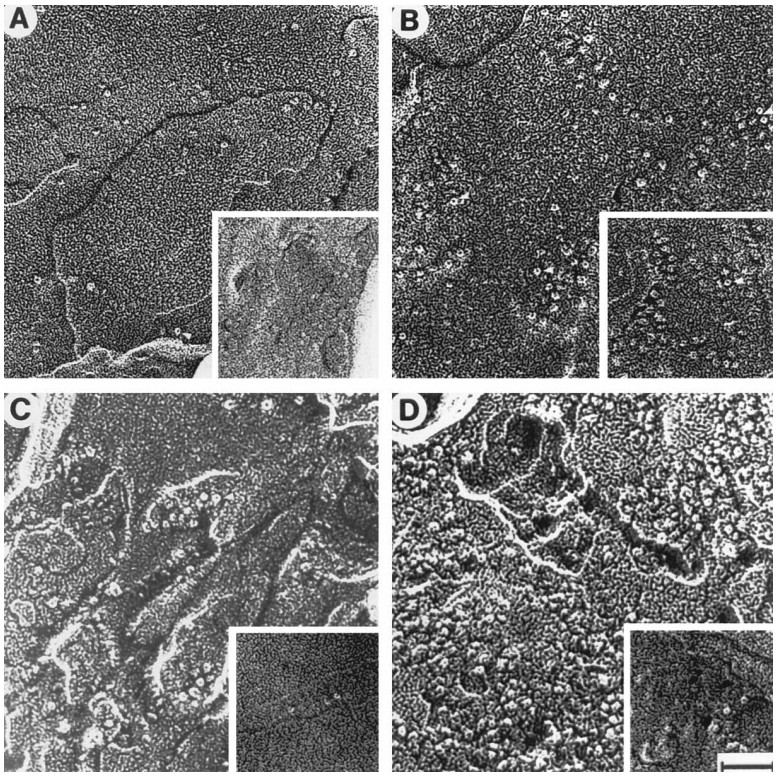

Figure 3. Freeze-Fracture Micrographs of the Sec61p Complex in Reconstituted Proteoliposomes

(A) Reconstituted canine Sec61p complex analyzed in the absence of ribosomes. The protein was reconstituted at ~100 pmol/100 μg lipid or at ~30 pmol/100 μg lipid (inset).

(B) Reconstituted canine Sec61p complex (~100 pmol/100 μg lipid) analyzed in the presence of wheat-germ ribosomes. The inset shows densely packed rings from a different specimen.

(C) Reconstituted Sec61p complex from S. cerevisiae analyzed in the presence or absence (inset) of yeast ribosomes.

(D) Reconstituted Sec61p complex from yeast, isolated from the dissociated heptameric Sec complex, analyzed in the presence or absence (inset) of yeast ribosomes. Scale bar = 500 Å.

were also observed with unstained samples, supporting the hypothesis that the Sec61p oligomers have an inherent degree of structural flexibility.

An estimate of the number of Sec61p heterotrimers per ring was obtained from the calculated volume of the particles. Although most molecules were viewed face-on, presumably because of their high affinity in this orientation for the carbon-film grids used for microscopy, some edge views of molecules were obtained in ice-over holes (not shown), giving a thickness of ~50–60 Å. Assuming a cylindrical particle with a diameter of 85 Å and a central pore of 20 Å, and using a partial specific volume of 0.73 cm^3/g for the protein, an estimate of 250 kDa was obtained, corresponding to 3–4 Sec61p heterotrimers per oligomer. An independent confirmation of this estimate was obtained by scanning-transmission electron microscopy analysis. In this method, the diffraction of electrons under conditions of dark-field imaging gives a measure of the particle mass (Wall and Hainfeld, 1986). The obtained mass average of 231 kDa (n = 270 molecules) suggests that one oligomer contains three Sec61p heterotrimers. However, the background values were roughly 25% higher than for comparable samples applied in buffers without detergent. If one assumes a theoretical background value, the mass is calculated to be ~280 kDa, consistent with either a trimer or tetramer of Sec61p complexes. Based on the number of peaks (4) in the two-dimensional maps, estimates from volume calculations (3–4 copies), scanning-transmission electron microscopy mass analysis (3–4 copies), and a determination of the molar ratio of Sec61p complexes relative to salt-resistant, ER-bound ribosomes (~4; see Discussion and Experimental Procedures), we estimate 3–4 heterotrimers per Sec61p oligomer.

In addition to the mammalian and yeast Sec61p complexes, we analyzed the purified heptameric Sec complex from yeast (Panzner et al., 1995). When viewed in digitonin by negative-stain electron microscopy, the Sec complex showed globular particles with an average diameter of ~105 Å (see the low magnification view in Figure 2B). Ring-like morphologies were absent; instead, in favorable orientations, the particles are asymmetrical with an off-center, stain-filled pore (see the arrowheads in Figure 2C).

Oligomers of the Sec61p Complex in Reconstituted Membranes

Next, we analyzed the Sec61p complex in reconstituted membrane vesicles to determine whether oligomers were present with a morphology similar to those seen in detergent. Freeze-fracture electron microscopy was employed to provide a view of the membrane surface and the interior of the phospholipid bilayer. Purified Sec61p complexes of dog pancreas and yeast were reconstituted into proteoliposomes, and the samples were quickly frozen and fractured to generate preferential cleavage planes within the bilayer. After etching at −100°C to make surface structures more visible, metal-carbon replicas were produced and viewed by electron microscopy. To our surprise, when the Sec61p complex was present in reconstituted proteoliposomes at approximately physiological concentrations, ring-like oligomers were generally absent (at most, 10 rings per μm^2; see the inset in Figure 3A), which was much rarer than expected from the experiments with solubilized complexes. However, the rings that could be seen were similar in size and structure to those in detergent. At high concentrations of the Sec61p complex in reconstituted

Table 1. Particle Sizes in Freeze-Fractured Membranes

Membranes	Mean Diameter (Å)	Standard Deviation (Å)	Number of Measurements
Rough microsomes	100	12.9	294
Ribosome-stripped microsomes	97.4	10.5	302
Reconstituted microsomes + ribosomes	111.5	12	112
Yeast nuclear envelopes	101.4	12.2	757
All "native" membranes	101	3.4	1465
Canine Sec61p complex + ribosomes	86.1	9.9	325
Yeast Sec61p complex + ribosomes	90	10.8	80
Yeast Sec61p complex + Sec62/63p complex	89.7	8.8	240
Yeast Sec complex	83	9.8	349
all proteoliposomes with purified complexes	86.2	2.8	994

proteoliposomes, a moderate number of ring-like structures were observed (Figure 3A; up to 60 rings per μm^2). Since rings were readily observed with the Sec61p complex in detergent, even at higher dilutions, it appeared that reconstitution of the Sec61p complex into phospholipid bilayers led to their dissociation.

We reasoned that reassembly of oligomeric Sec61p rings in the plane of the membrane might be stimulated by natural effectors of the translocation process. In the cotranslational pathway, ribosomes might induce oligomerization since they are known to interact tightly and specifically with the Sec61p complex (Kalies et al., 1994; Jungnickel and Rapoport, 1995). Indeed, when isolated wheat-germ ribosomes lacking nascent polypeptide chains were added to proteoliposomes containing the purified canine Sec61p complex, a significant increase in the number of rings (up to 600 per μm^2) was seen in freeze fracture (Figure 3B). The oligomers had a quasi-pentagonal appearance with an average diameter of 86 Å (see Table 1), similar to those seen in detergent solution. Such structures were not observed in control vesicles lacking the Sec61p complex (not shown). Rings were also formed in large numbers (up to 500 per μm^2) when yeast ribosomes were added to proteoliposomes containing yeast Sec61p complex, purified either as a heterotrimer from yeast microsomes (Figure 3C) or after dissociation of the purified heptameric Sec complex involved in posttranslational translocation (Panzner et al., 1995) (Figure 3D). In each case, proteoliposomes incubated without ribosomes showed less than 60 ring structures per μm^2 (see the insets in Figures 3C and 3D). Therefore, we conclude that the ribosome, a natural ligand of the Sec61p complex in cotranslational protein transport, can induce oligomerization of the Sec61p complex in the plane of the membrane. Furthermore, since the free Sec61p complex from yeast microsomes and that contained in the heptameric Sec complex were responsive to ribosomes, one may assume that the same Sec61p complex can function in co- and post-translational translocation pathways.

Next, we tested whether the Sec62/63p complex, whose association with the Sec61p complex is essential for the posttranslational pathway of protein transport (Panzner et al., 1995), would also induce oligomeric ring structures. When the Sec61p complex or the Sec62/63p complex, both isolated after dissociation of the heptameric Sec complex, were reconstituted separately into proteoliposomes at approximately the same concentrations and analyzed by freeze-fracture electron microscopy, rings were not observed (see Figures 4A and 4B). However, when the subcomplexes were recombined during reconstitution, rings appeared in large numbers (Figure 4C). Virtually every fracture face showed small patches of polygonal rings that were indistinguishable from those seen with the original, nondissociated Sec complex (Figure 4D and Table 1). Taken together, these results indicate that the formation of oligomeric rings of the Sec61p complex can be mediated by either ribosomes or the Sec62/63p membrane protein complex.

Oligomers of the Sec61p Complex in Native ER Membranes

If the oligomeric rings of the Sec61p complex observed in detergent and in reconstituted membranes have physiological relevance, they should also be visible in native rough ER membranes. Indeed, when freeze-fracture electron microscopy was used to analyze canine rough microsomes (RM), internal fracture planes showed intramembranous particles with the characteristic polygonal ring morphology (Figure 5A and inset). Quantitation demonstrated that the particles have an average diameter of 100 Å (see Table 1) and are present at a density of ~200–300/μm^2. The latter may be a lower estimate of the actual number of rings because not all particles may be visible if incompletely covered by metal, and some particles may have been peeled off with either the membrane leaflet or the ribosomes. On the cytoplasmic surface of the vesicles, ribosomes were readily visible as ~250 Å diameter bumps (in Figure 5A, see the region marked R in the upper left corner). The density of ribosomes was estimated to be ~900–1100/μm^2, in reasonable agreement with determinations based on absorption at 260 nm of the microsomes and on their lipid content.

Oligomeric rings were also observed by freeze fracture in yeast nuclear envelopes, which are contiguous with the ER (Figure 6). As with mammalian microsomes, the internal fracture faces were densely covered with polygonal rings (Figures 6B and 6C; density ~380/μm^2) with an average diameter of 101 Å (see Table 1), although some larger ring-like structures could also be seen (Figure 6C). As expected, the cytoplasmic surface of the nuclear envelopes was covered with bound ribosomes (Figure 6A; density ~550/μm^2). Figures 6A and 6B are shown at the same magnification to allow a direct comparison of the size of the ribosomes (arrow labeled R; ~250 Å diameter) and the rings.

Surprisingly, the removal of ribosomes from the mammalian ER membranes by treatment with puromycin and

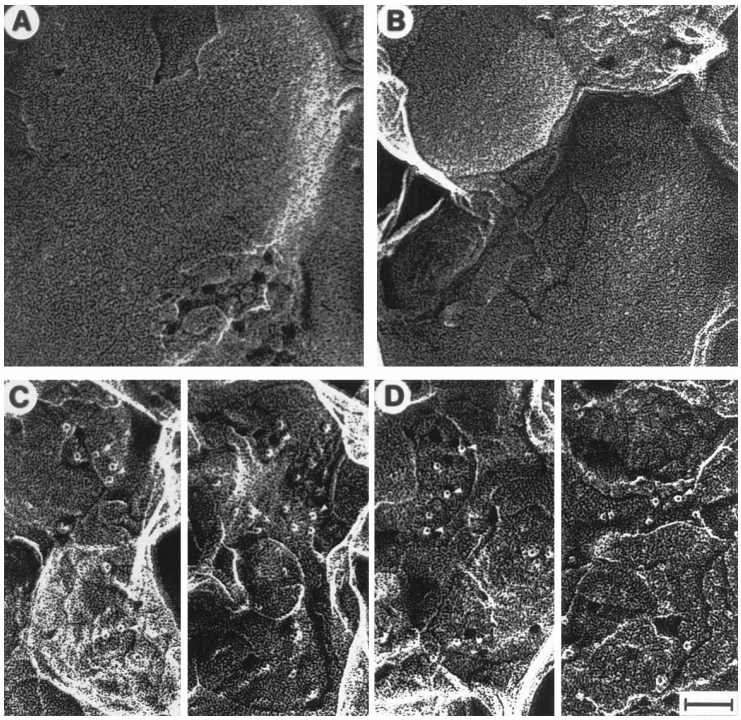

Figure 4. Freeze-Fracture Micrographs of the Heptameric Sec Complex from Yeast and Its Subcomplexes in Reconstituted Proteoliposomes

(A) Reconstituted yeast Sec61p subcomplex, isolated from the dissociated heptameric Sec complex.

(B) Reconstituted yeast Sec62/63p subcomplex, isolated upon dissociation of the heptameric Sec complex.

(C) Coreconstitution of the yeast Sec61p and Sec62/63p subcomplexes.

(D) Reconstitution of the native heptameric Sec complex. Scale bar = 500 Å.

high-salt concentrations did not result in a significant reduction of the number of ring structures (Figure 5B), raising the question as to whether they are formed by Sec61p. To test this, proteoliposomes were produced from a digitonin extract of ribosome-stripped microsomes, with and without immunodepletion of the Sec61p complex (Kutay et al., 1995), and analyzed by freeze-fracture electron microscopy. In nondepleted proteoliposomes analyzed in the presence (Figure 5C) or absence of ribosomes (not shown), a large number of ring structures with the characteristic morphology and diameter of those in native membranes was observed (also see Table 1). In the Sec61p-depleted proteoliposomes, the number of ring structures was greatly reduced, even after the addition of ribosomes (Figures 5E and 5F). Mock-depleted proteoliposomes showed an undiminished number of ring structures (Figure 5D). Therefore, we conclude that the ring structures in native membranes depend mostly, if not entirely, on the presence of the Sec61p complex.

Discussion

We have used electron microscopy to provide the first structural view of the Sec61p complex, the main component of the protein translocation apparatus of the ER membrane and the most probable candidate to form the aqueous channel through which proteins cross the membrane. In detergent, this heterotrimeric membrane protein complex forms cylinders with a quasipentagonal appearance and a central pore. Each ring contains 3–4 molecules of the Sec61p complex. Ring-like oligomers of the Sec61p complexes from mammals and yeast are strikingly similar in shape and size, reinforcing conclusions drawn from primary sequence data that the translocation apparatus of the ER membrane is evolutionarily highly conserved (Hartmann et al., 1994). Ring structures of the Sec61p complex are also seen in reconstituted and native membranes. Their formation is induced in reconstituted membranes by the addition of ribosomes, essential ligands in cotranslational translocation. Similar oligomeric ring structures are produced when the Sec61p complex interacts in the membrane with the Sec62/63p complex, an association that is required for posttranslational protein transport in a purified system (Panzner et al., 1995). Our data suggest that in the posttranslational mode of translocation, a membrane protein complex replaces the function of the ribosome in inducing the formation of oligomers of the Sec61p complex. We propose that these oligomeric ring structures represent the elusive protein-conducting channels of the ER membrane.

The best views of the ring structure formed by the Sec61p complex were obtained in detergent. The particles are cylinders with a diameter of ~85 Å, a height of ~50–60 Å, and a central pore with a diameter of ~20 Å. The quasipentagonal shape in projection may indicate that the 3–4 subunits are tilted differently around the ring, or that they are biochemically distinct (e.g., not all of them may contain the β subunit that is more easily dissociable). Freeze-fracture analysis of the Sec61p complex reconstituted into proteoliposomes produced a similar morphology for the oligomers, suggesting that they normally sit in the bilayer with their central pore aligned perpendicular to the plane of the membrane. In this orientation, their height would allow them to span the lipid bilayer completely. The central pore was observed in negatively stained and unstained specimens in detergent, and also in freeze fractures of the protein in membranes. However, it is not clear whether the central pore passes all the way through the membrane or is only a deep indentation closed at one end. For the complexes in detergent, we observed significant variation

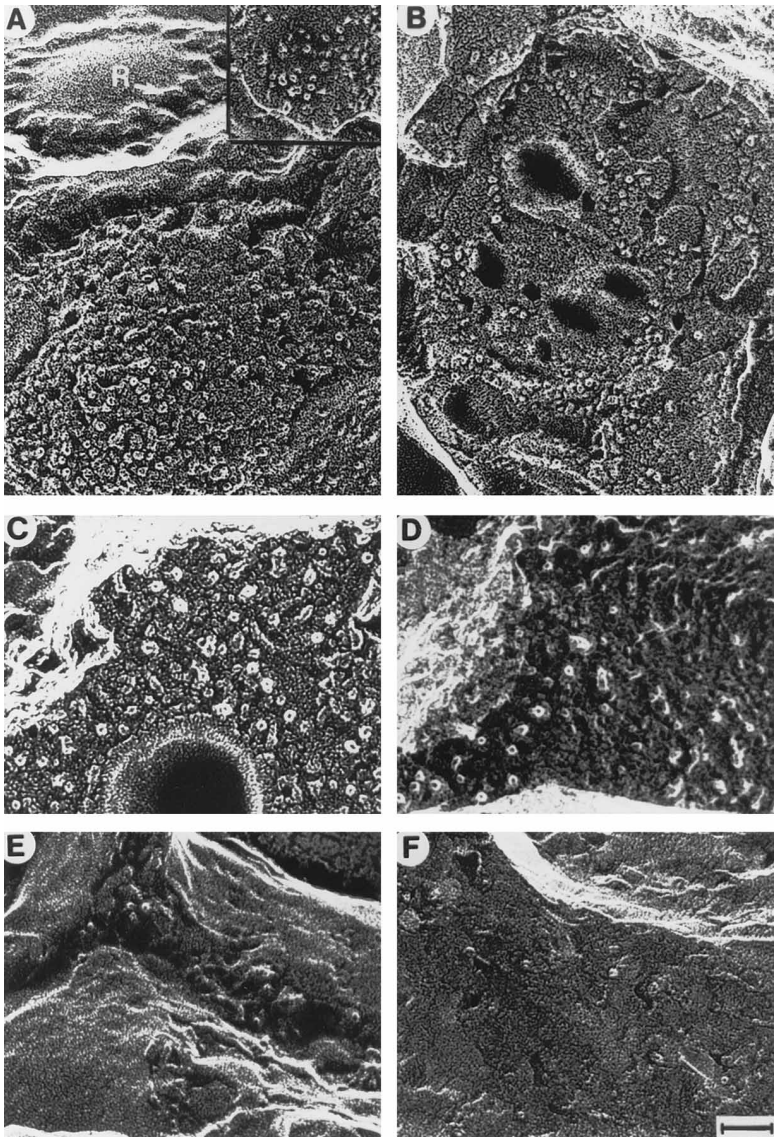

Figure 5. Freeze-Fracture Electron Micrographs of Native and Reconstituted Canine Microsomes

(A) Freeze-fracture and deep-etch faces from RM reveal ring-like particles and ribosome surface "bumps" (white arrow labeled R). Many of the rings have a quasipentagonal morphology (see arrowheads in the inset).

(B) Native microsomes stripped of ribosomes by treatment with puromycin/high salt.

(C) Proteoliposomes reconstituted from a crude digitonin extract of ribosome-stripped microsomes. The sample was analyzed in the presence of wheat-germ ribosomes.

(D) Proteoliposomes reconstituted from a crude extract that had been subjected to a mock depletion of the Sec61p complex. The sample was analyzed in the presence of wheat-germ ribosomes. (E) Proteoliposomes reconstituted from a crude extract that had been subjected to immunodepletion of the Sec61p complex. The sample was analyzed without ribosome addition.

(F) Proteoliposomes reconstituted from a crude extract that had been subjected to immunodepletion of the Sec61p complex. The sample was analyzed in the presence of ribosomes. Scale bar = 500 Å.

in the diameters of the molecule and its central pore that cannot be explained by different projections. Whether these observations reflect heterogeneity with respect to conformation, variable numbers of Sec61p heterotrimers per ring, differences in subunit composition, or variations in the number of bound detergent molecules is unknown.

The heptameric Sec complex from yeast, when viewed in detergent, did not show the ring-like morphology characteristic of the Sec61p subcomplex, although a subset of particles showed an off-center pore. The presence of the Sec62/63p complex may cause a loss of the preferential orientation of the cylindrical Sec61p that allows visualization of the pore in each particle. However, the Sec complex was very similar to the Sec61p heterotrimer when examined in reconstituted membranes by freeze fracture. This indicates that most of the mass provided by the four additional subunits is unlikely to be within the membrane and may instead be localized above and below the Sec61p cylinder.

Particles with a ring morphology, similar to that observed with the purified Sec61p complex, were observed by freeze-fracture analysis of native rough ER membranes of mammals and yeast. They had the quasipentagonal appearance that is characteristic of the structure of the purified complex and occurred at a frequency consistent with their being oligomers of the Sec61p complex (in canine microsomes, ~200–300 rings/μm^2 versus an estimated 900–1000 Sec61p complex molecules/μm^2). Furthermore, proteoliposomes that were depleted of the Sec61p complex, but which contained all other membrane proteins of the mammalian ER, gave a much reduced number of rings, indicating that most if not all of these structures require the Sec61p complex for formation. The size distribution of the particles in native membranes was centered on a larger average diameter than that of the reconstituted Sec61p oligomers (101 Å versus 86 Å). Since some large (101 Å) particles were also observed with the purified, reconstituted complex, these data reinforce the possibility

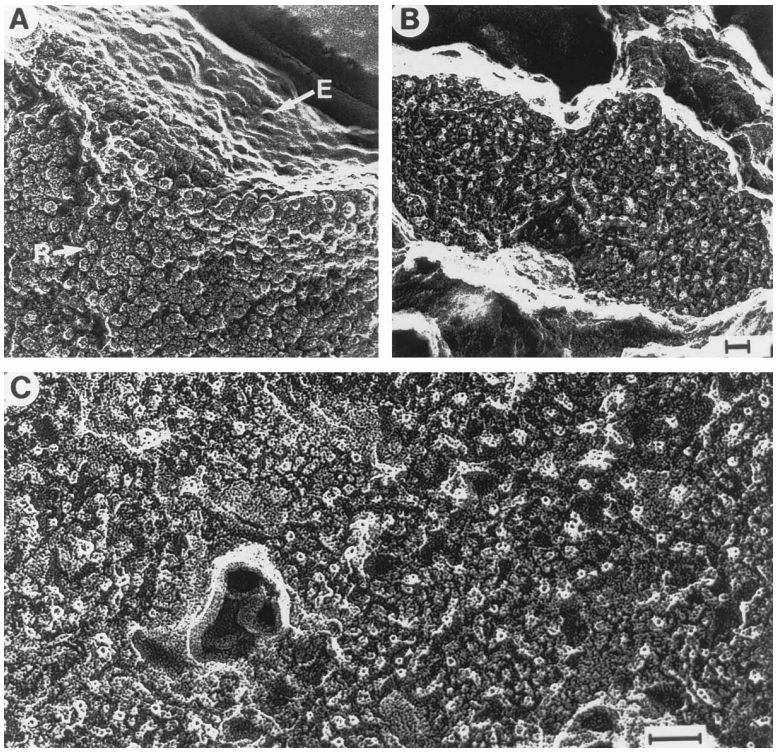

Figure 6. Freeze-Fracture Electron Micrographs of Yeast Nuclear Envelopes

(A) Cytoplasmic surface of the yeast nuclear envelopes, as viewed by deep etching to reveal ribosome "bumps" (upper surface, see the white arrow labeled E). The lower surface shows a rare fracture that occurred close to the outer nuclear-envelope surface and thereby revealed the ribosomes (see the arrow labeled R).

(B) A fracture plane revealing ring-like particles in the plane of the membrane. (A) and (B) are shown at the same scale (scale bar = 500 Å).

(C) A magnified region of an internal fracture face of the nuclear envelope. The arrowheads point to typical ring-like structures. Scale bar = 500 Å.

that the Sec61p oligomers can occur either in different conformations or with a different number of subunits. The observed rings are most likely identical to particles seen previously in large numbers by freeze fracture of rat liver RMs (average diameter: ~105 Å) (Ojakian et al., 1977) and in the ER of the green alga Micrasterias denticulata (110 Å ± 17 Å) (Giddings and Staehelin, 1980). Significantly, in the case of the green alga, one of these particles was under each ribosome within spiral polysomes containing 15–20 ribosomes. Given that the 110 Å particles are likely to be comprised of the Sec61p complex, these results suggest that the oligomerized state of the Sec61p complex may be maintained throughout the translocation process. Although it is not clear why the intramembranous particles were not seen as quasipentagonal rings in the previous work, use of glycerol or high concentrations of other low molecular weight compounds may have masked details of this morphology. The prolonged deep etching and the rotary shadowing with metal employed in the present work may also have allowed a clearer visualization of the particles. In particular, the quasipentagonal morphology cannot be attributed to an artifact of rotary shadowing. Although a visualization of the central pore may be enhanced significantly by this treatment, the striking agreement with the results obtained with particles in detergent strongly supports the existence of a pore.

We propose that oligomers of the Sec61p complex form the protein-conducting channels of the ER membrane. The central pore in the cylindrical oligomer potentially provides the extended aqueous environment, bounded by Sec61p, in which the nascent chain has been detected by electrophysiological, fluorescence, and cross-linking experiments. This would be consistent with all data that demonstrate an essential and evolutionarily conserved role for the Sec61p complex in translocation and would explain why similar rings are induced by effectors of the co- and posttranslational pathways. The diameter of the pore (~20 Å) is smaller than the minimum estimate (30 Å) made from fluorescence-quenching experiments (A. Johnson, personal communication). However, our values obtained from the projection of negatively stained and unstained purified complexes in detergent may represent a lower estimate. Moreover, it is possible that the channel is viewed in its closed state (see below).

If the Sec61p rings in native membranes represent ribosome-associated channels, one would predict at least a 3- to 4-fold molar excess of Sec61p complex molecules over ribosomes engaged in translocation. Our quantitations (see Experimental Procedures) indicate that rough microsomes from canine pancreas contain 1.50 ± 0.09 (n = 7) pmol ribosomes/equivalent membranes, but that only 0.39 ± 0.04 (n = 7) pmol/equivalent (26%) are bound in a high salt-resistant manner, characteristic of ribosomes engaged in translocation. The same membranes contain 1.67 ± 0.16 (n = 3) pmol Sec61p complex/equivalent, which is clearly sufficient to account for a 3- to 4-fold stoichiometry with respect to the tightly bound ribosomes. Ribosome-binding experiments with ribosome-stripped membranes, carried out at physiological salt concentrations, give 0.27–0.30 pmol binding sites/equivalent, and most if not all of these can be attributed to the Sec61p complex (Kalies et al., 1994). Although these data are consistent with oligomers of 3–4 Sec61p complexes forming channels, they suggest that many ribosomes in RM are not engaged in translocation.

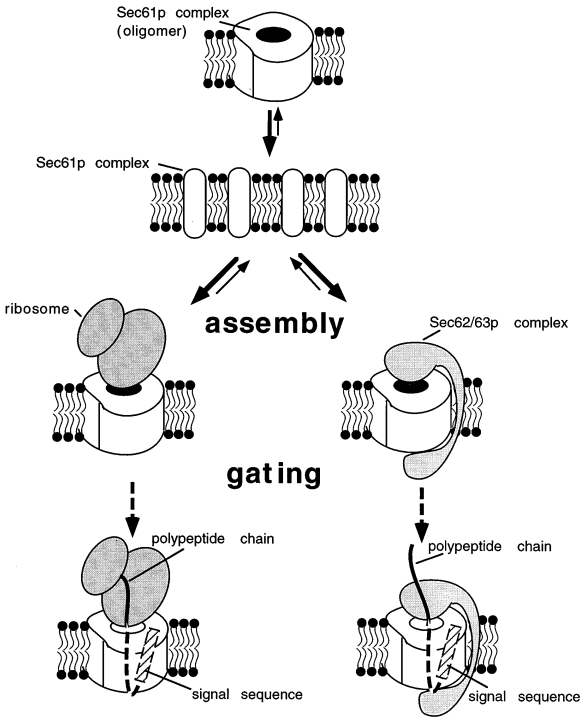

Figure 7. Model for the Role of an Oligomer of the Sec61p Complex in Protein Translocation Across the ER Membrane

In the model shown, an equilibrium exists between monomeric and oligomeric Sec61p heterotrimers that favors monomers in the absence of the appropriate ligands. In the cotranslational pathway, the binding of the ribosome would stimulate assembly of oligomers. In the posttranslational pathway, the role of the ribosome would be replaced by the Sec62/63p complex. In both cases, the channel would initially be closed and only opened upon interaction with the signal sequence of a translocating polypeptide chain (gating). In an alternative model, the ribosome or the Sec62/63p complex would bind directly to a previously assembled Sec61p oligomer. The gating step would remain unchanged.

The ability of the ribosome to induce oligomers of the Sec61p complex suggests the possibility that the channel is assembled de novo during each round of cotranslational translocation. In this model (Figure 7), the Sec61p complex would be in the monomeric form in the absence of translocation because the assembly equilibrium favors the monomer at physiological concentrations. During initiation of translocation, the ribosome would shift this equilibrium to the oligomerized form, perhaps by initially interacting with only one molecule of the Sec61p complex, which would then nucleate oligomerization. Conceivably, the signal recognition protein receptor could also play a role in this assembly reaction and other proteins, such as translocating chain-associating membrane, the signal peptidase, or the oligosaccharyl transferase, may be recruited to the translocation site because of preferential associations with the oligomeric state of the Sec61p complex. An interaction between the nascent chain and the Sec61p complex may not be required for initial oligomerization but may come into play only at a later step. This view is supported by the fact that ribosomes carrying short nascent chains are initially bound in a salt- and protease-sensitive manner to the Sec61p complex, and only upon further elongation of the polypeptide chain is a second, more tightly bound stage achieved (Jungnickel and Rapoport, 1995; Belin et al., 1996). The transition between these stages requires a functional signal sequence and takes place at the same chain length at which fluorescence-quenching agents indicate that the channel opens (Crowley et al., 1994; Jungnickel and Rapoport, 1995). Taken together, these results suggest a model in which assembly and gating of the protein-conducting channel are consecutive and distinct events during initiation of cotranslational translocation (Figure 7): the channel structure is induced by the binding of the ribosome to the Sec61p complex but is opened only upon subsequent interaction with the signal sequence of the nascent chain.

In an alternative model, the channel would stay assembled for more than one round of translocation, possibly throughout its lifetime. This view is supported by the fact that membranes stripped of ribosomes by puromycin/high salt treatment, as well as proteoliposomes reconstituted from them after detergent solubilization, still show large numbers of Sec61p oligomers. Others have made similar observations (Ojakian et al., 1977). Since disassembly of oligomers during reconstitution was observed with the purified Sec61p complex but not with the complex in a crude mixture, the oligomeric form may be stabilized by other membrane proteins even after removal of the ribosome. However, it is possible that during physiological termination of translocation, the stabilizing influence exerted by other components may be inactivated, causing disassembly of the channel.

Similar models can be envisioned for the posttranslational mode of transport. The Sec62/63p complex may cause assembly of the Sec61p oligomers during each round of translocation or may stay assembled with them permanently. Since the heptameric Sec complex can be purified as a unit (Panzner et al., 1995), it may constitute a stable, closed channel structure, opened only upon interaction with the signal sequence of a potential substrate (Figure 7).

The possibility that assembly and gating occur in an independent and consecutive manner in co- and posttranslational transport would allow the membrane barrier to be maintained even though the channel can be assembled in the absence of a nascent chain. A separate gating event would also explain why puromycin/high-salt treatment of RM is sufficient to close the channels in electrophysiological experiments (Simon and Blobel, 1991) but insufficient to cause their disassembly, as we have observed by electron microscopy.

Finally, formation of the protein-conducting channel by a weak association of subunits within the plane of the membrane potentially provides a mechanism for translocating nascent chains to sample hydrophilic and lipid environments. One or more of the subunit interfaces could open transiently, allowing the nascent chain to intercalate between the subunits and test the hydrophobic environment of the phospholipid bilayer. Indeed, experimental evidence suggests that hydrophobic segments of a nascent chain are located in a position that allows them to contact Sec61α and lipid (Martoglio et al., 1995). Movement between adjacent subunits would

provide a mechanism by which transmembrane segments of integral membrane proteins could exit the channel (Singer et al., 1987; Simon and Blobel, 1991), and the asymmetric design may destabilize a particular subunit interface, allowing it to act as a lateral gate.

Experimental Procedures

Preparation of Mammalian Membranes

Dog pancreatic RM were prepared by the procedure of Walter and Blobel (1983). Puromycin- and high salt-washed RM were prepared as described by Kalies et al. (1994). This resulted in the removal of at least 90% of the ribosomes, as judged from the absorption at 260 nm.

Preparation of Yeast Nuclear Membranes

Yeast nuclear envelope preparations were carried out as described by Strambio-de-Castillia et al. (1995). The samples were dialyzed overnight against 10 mM Tris–HCl (pH 6.8), 0.75 mM $MgCl_2$, and 4% dimethyl sulfoxide, centrifuged at 20,000 rpm for 20 min in a mini-Sorval RP-55S and resuspended in 10 μl of the same buffer without dimethyl sulfoxide before freezing.

Purification of Protein Complexes

The canine trimeric Sec61p complex was purified from either the ribosome-associated membrane protein fraction of RM, or from puromycin- and high salt-washed RM (Görlich and Rapoport, 1993). The yeast heptameric Sec complex was purified by the peptide antibody affinity procedure as described by Panzner et al. (1995), with the omission of the saponin-extraction step. Dissociation of the Sec complex into its component Sec61p and Sec62/63p complexes was as described in the same reference. Purification from yeast of the free trimeric Sec61p complex was as described by Finke et al. (1996), using the concanavalin A flow-through fraction of the nonribosome-associated proteins as starting material. Detergent exchange for reconstitution was performed on a 300 μl S-Sepharose spin column equilibrated with 50 mM HEPES–KOH (pH 7.5), 0.3% deoxyBigCHAP, 5 mM 2-mercaptoethanol, and 10% (w/v) glycerol; elution was carried out with the same buffer containing 450 mM KOAc.

Reconstitution of Protein Complexes into Proteoliposomes

Reconstitution of the mammalian Sec61p complex was performed in 13 μl with 30–100 pmol of Sec61p and 100 μg of a lipid mixture (phosphatidylcholine, phosphatidylethanolamine, phosphatidylinositol, and phosphatidylserine in the weight ratios of 68:20:10:2) using Biobeads SM2 for detergent removal (Görlich and Rapoport, 1993). Reconstituted proteoliposomes were collected by centrifugation and resuspended in 5 μl of 50 mM HEPES–KOH (pH 7.5), 100 mM KOAc, and 2 mM magnesium acetate.

All complexes derived from yeast were reconstituted as described in Panzner et al. (1995), using Biobeads SM2 and a mixture of phosphatidylcholine and phosphatidylethanolamine in a weight ratio of 4:1. After reconstitution, proteoliposomes were collected by diluting the liquid above the beads 20- to 30-fold with 30 mM HEPES–KOH (pH 7.5), 40 mM KOAc, and 1 mM dithiothreitol (DTT), followed by centrifugation for 45 min at 75,000 rpm and 20°C in a TL100.3 rotor (Beckman). The pellet was resuspended in the same buffer. For freeze-fracture electron microscopy of the yeast Sec complex, reconstitutions were carried out in 20 μl containing ~112 μg of lipid and 8 pmol of Sec61p in the heptameric complex, and 12 pmol of Sec61p or Sec63p in the dissociated and recombined subcomplexes. For experiments involving ribosome treatment of proteoliposomes, a 25 μl reconstitution contained 20 μg of lipid and 38 pmol of yeast Sec61p complex.

Preparation of Ribosomes

Ribosomes were prepared from a wheat-germ extract as described (Jungnickel and Rapoport, 1995) and resuspended in 50 mM HEPES–KOH (pH 7.5), 150 mM KOAc, and 2 mM magnesium acetate. Yeast ribosomes used with yeast complexes were prepared by the procedure of Deshaies and Kirschner (1995). To 0.1 ml extract were added 0.9 ml of 40 mM HEPES–KOH (pH 7.5), 500 mM KOAc, 5 mM magnesium acetate, 2 mM DTT, and the ribosomes collected by centrifugation (100,000 rpm, 40 min, 20°C, TL 100.3 rotor, Beckman) through a 2 ml cushion of 500 mM sucrose in the same buffer used for dilution. The ribosomal pellet was resuspended in 20 mM HEPES–KOH (pH 7.5), 150 mM KOAc, 2 mM magnesium acetate, and 2 mM DTT.

Incubation of Membranes with Ribosomes

Ribosome binding to reconstituted proteoliposomes was performed as described (Jungnickel and Rapoport, 1995). Final binding conditions for mammalian components were 50 mM HEPES–KOH (pH 7.5), 125 mM KOAc, 2 mM magnesium acetate, with 5–12 μM Sec61p and ~350 nM ribosomes. Final binding conditions with yeast components were 25 mM HEPES–KOH (pH 7.5), 95 mM KOAc, 1 mM magnesium acetate, and 0.5 mM DTT, with ~4 μM Sec61p and 850 nM ribosomes. For puromycin- and high salt-washed RM and reconstituted proteoliposomes produced from crude detergent extracts, 0.5–1.5 equivalents/μl and ~350 nM ribosomes were used. The reactions were first incubated on ice for 10 min and then at 27°C for 5 min, after which they were quickly frozen and processed for electron microscopy.

Proteoliposomes Depleted of the Sec61p Complex

Reconstitutions from a 1% digitonin extract of canine puromycin- and high salt-washed RM after immunodepletion of the Sec61p complex with immobilized antibodies directed against the β subunit of the complex was carried out as described (Kutay et al., 1995). Depletion was approximately 95%, as determined by immunoblotting with affinity-purified antipeptide antibodies against the α and β subunits of the complex. Mock depletion experiments were performed with the same quantities of protein A/G-Sepharose beads.

Quantitation of Ribosomes and Sec61p Complex in Canine Microsomes

The number of ribosomes in 1 equivalent RM (defined in Walter et al., 1981) was determined after solubilization of the membranes in a buffer containing 25 mM HEPES–KOH (pH 7.6), 500 mM KCl, 10 mM $MgCl_2$, 100 mM sucrose, 1 mM DTT, and 1.8% digitonin, and sedimentation of the ribosomes. One unit of A260nm was taken to correspond to 16 pmol of ribosomes. The number of ribosomes bound to the membranes in a high salt-resistant manner was determined after treatment with 0.5 M CsCl, followed by flotation of the membranes. The amount of Sec61p complex in 1 equivalent of RM was determined by quantitative immunoblotting, using antibodies against the α or β subunit (which gave almost identical results, assuming a 1:1 stoichiometry) and ^{35}S-labeled secondary antibodies.

Electron Microscopy

For negative staining, Sec61p complexes (1–100 μg/ml) were applied to fresh, air-glow discharged carbon grids (400-mesh copper) as ~4–6 μl drops and incubated at 4°C for ~45 min. Samples were then fixed briefly (1–2′) in a buffer that maintained the salt and detergent composition of the original sample and contained 4% formaldehyde/0.5% glutaraldehyde. They were blotted to remove excess liquid, serially rinsed with 10–12 drops of 4% uranyl acetate, and air-dried. Minimal-dose electron microscopy was performed at 100 kV on a Philips CM12 transmission electron microscope equipped with a low dose kit and LaB6 filament using a defocus of 1–2 μm. For cryoelectron microscopy, Sec61p complexes were applied to n-amylamine treated or air-glow discharged holey carbon grids (400-mesh) in a humidified chamber, blotted, and plunged into liquid ethane (Dubochet et al., 1988). A Gatan cryotransfer system and coldholder (model 626-DH) were used to transfer grids to a Philips CM12 electron microscope equipped with a cryoblade-type anticontaminator. Most images were photographed at a magnification of 60,000× on Kodak SO163 film and developed for 12′ in full-strength D19 developer (Kodak). The powder diffraction images were recorded at 22,000×.

Image Processing and Classification

A series of micrographs in which the distribution of particles and stain appeared similar was chosen for image processing. Digitization was done on an Eikonics scanner at a step size of 4.0 Å/pixel (negative stain) or 3.25 Å/pixel (ice) and subsequently scaled to the same magnification. Image processing was done using the SPIDER software package (Frank et al., 1996). The procedure of cross-correlational alignment, averaging, and classification techniques, as applied to single particles, has been described (Frank et al., 1988; Akey, 1995). Specifically, after an initial round of alignment to check for handedness, we used the reference-dependent alignment effect to boost the signal-to-noise ratio in individual negatively stained Sec61p complexes. A miniature multireference alignment was first carried out in which every particle served as a reference against its 20 nearest neighbors. These enhanced averages (n = 543) were then used to determine the up-down orientations of the particles. Of the best single particles determined by this technique, 10–12 were used for a full multireference alignment against the entire data set. These final multireference averages were then aligned and averaged to form global averages. The aligned 20-fold averaged particle series was also used for classification. Our analysis excluded the smaller fragments and occasional rings of a diameter larger than 100 Å.

Freeze-Fracture Electron Microscopy

Concentrated membrane samples were frozen on copper hat supports by hand plunging into liquid Freon-22. After storage under liquid nitrogen, specimens were fractured at −100°C in a Balzers BAF-400 freeze-etching device and etched at high vacuum for 5–7 min. Replicas were prepared by rotary shadowing with platinum at an angle of 22° (~5 Å thick), followed by carbon shadowing at an angle of 90° (~35 Å thick). Successful replicas were cleaned with chromic acid and then washed with water before examination at 120 kV at 60,000× in a Philips CM12 electron microscope. The diameters of intramembranous particles visible in fracture faces were measured using a 10× magnifier equipped with a calibrated micrometer grating, rounding values to the nearest tenth of a millimeter.

Mass Analysis

Mass analysis of the canine Sec61p complex was performed on the scanning-transmission electron microscopy I unit at Brookhaven National Laboratory (Wall and Hainfeld, 1986), using tobacco mosaic virus as an internal standard. To analyze the small particles, the standard mass scan was converted to SPIDER-image format, and individual particles were selected in the WEB viewer (Frank et al., 1996). SPIDER routines were written to calculate the integrated particle density after background subtraction, and the tobacco mosaic virus scale factor was calculated in the Brandeis mass-analysis program (provided by Dr. G. Sosinsky).

Acknowledgments

This work was supported by NIH grants to C. W. A. and T. A. R., the Fulbright Junior Research Program (D. H.), and a Rothschild Fellowship (D. H.). We thank Dr. J. Wall and M. Simon for collecting scanning-transmission electron microscopy images analyzed in this work, and Dr. E. Bullitt for help with the Brandeis mass-analysis programs. We thank M. Rolls, P. Stein, and E. Hartmann for critical reading of the manuscript.

Received August 22, 1996; revised September 24, 1996.

References

Akey, C.W. (1995). Structural plasticity of the nuclear pore complex. J. Mol. Biol. *248*, 273–293.

Belin, D., Bost, S., Vassalli, J.-D., and Strub, K. (1996). A two-step recognition of signal sequences determines the translocation efficiency of proteins. EMBO J. *15*, 468–478.

Blobel, G., and Dobberstein, B. (1975). Transfer of proteins across membranes. II. Reconstitution of functional rough microsomes from heterologous components. J. Cell Biol. *67*, 852–862.

Crowley, K.S., Reinhart, G.D., and Johnson, A.E. (1993). The signal sequence moves through a ribosomal tunnel into a noncytoplasmic aqueous environment at the ER membrane early in translocation. Cell *73*, 1101–1115.

Crowley, K.S., Liao, S.R., Worrell, V.E., Reinhart, G.D., and Johnson, A.E. (1994). Secretory proteins move through the endoplasmic reticulum membrane via an aqueous, gated pore. Cell *78*, 461–471.

Deshaies, R.J., and Kirschner, M. (1995). G1 cyclin-dependent activation of p34CDC28 (Cdc28p) in vitro. Proc. Natl. Acad. Sci. USA *92*, 1182–1186.

Deshaies, R.J., and Schekman, R. (1987). A yeast mutant defective at an early stage in import of secretory protein precursors into the endoplasmic reticulum. J. Cell Biol. *105*, 633–645.

Do, H., Falcone, D., Lin, J., Andrews, D.W., and Johnson, A.E. (1996). The cotranslational integration of membrane proteins into the phospholipid bilayer is a multistep process. Cell *85*, 369–378.

Dubochet, J., Adrian, M., Chang, J.-J., Homo, J.-C., Lepault, J., McDowall, A.W., and Schultz, P. (1988). Cryo-electron microscopy of vitrified specimens. Q. Rev. Biophys. *21*, 129-228.

Finke, K., Plath, K., Panzner, S., Prehn, S., Rapoport, T.A., Hartmann, E., and Sommer, Th. (1996). A second trimeric complex containing homologs of the Sec61p-complex functions in protein transport across the ER membrane of S. cerevisiae. EMBO J. *15*, 1482–1494.

Frank, J., Bretaudiere, J.-P., Carazo, J.-M., Verschoor, A., and Wagenknecht, T. (1988). Classification of images of biomolecular assemblies: a study of ribosomes and ribosomal subunits of Escherichia coli. J. Microscopy *150*, 99–115.

Frank, J., Radermacher, M., Penczek, P., Zhu, J., Li, Y., Ladjadj, M., and Leith, A. (1996). SPIDER and WEB: processing and visualization of images in 3D electron microscopy and related fields. J. Struct. Biol. *116*, 190–199.

Giddings, T.H., and Staehelin, L.A. (1980). Ribosome binding sites visualized on freeze-fractured membranes of the rough endoplasmic reticulum. J. Cell Biol. *85*, 147–152.

Görlich, D., Prehn, S., Hartmann, E., Kalies, K.U., and Rapoport, T.A. (1992). A mammalian homolog of SEC61p and SECYp is associated with ribosomes and nascent polypeptides during translocation. Cell *71*, 489–503.

Görlich, D., and Rapoport, T.A. (1993). Protein translocation into proteoliposomes reconstituted from purified components of the endoplasmic reticulum membrane. Cell *75*, 615–630.

Hartmann, E., Sommer, T., Prehn, S., Görlich, D., Jentsch, S., and Rapoport, T.A. (1994). Evolutionary conservation of components of the protein translocation complex. Nature *367*, 654–657.

High, S., Andersen, S.S.L., Görlich, D., Hartmann, E., Prehn, S., Rapoport, T.A., and Dobberstein, B. (1993). Sec61p is adjacent to nascent type I and type II signal-anchor proteins during their membrane insertion. J. Cell Biol. *121*, 743–750.

Jungnickel, B., and Rapoport, T.A. (1995). A posttargeting signal sequence recognition event in the endoplasmic reticulum membrane. Cell *82*, 261–270.

Kalies, K.U., Görlich, D., and Rapoport, T.A. (1994). Binding of ribosomes to the rough endoplasmic reticulum mediated by the sec61p-complex. J. Cell Biol. *126*, 925–934.

Kellaris, K.V., Bowen, S., and Gilmore, R. (1991). ER translocation intermediates are adjacent to a nonglycosylated 34-kD integral membrane protein. J. Cell Biol. *114*, 21–33.

Kutay, U., Ahnert-Hilger, G., Hartmann, E., Wiedenmann, B., and Rapoport, T.A. (1995). Transport route for synaptobrevin via a novel pathway of insertion into the endoplasmic reticulum membrane. EMBO J. *14*, 217–223.

Martoglio, B., Hofmann, M.W., Brunner, J., and Dobberstein, B. (1995). The protein-conducting channel in the membrane of the endoplasmic reticulum is open laterally toward the lipid bilayer. Cell *81*, 207–214.

Mothes, W., Prehn, S., and Rapoport, T.A. (1994). Systematic probing of the environment of a translocating secretory protein during translocation through the ER membrane. EMBO J. *13*, 3937–3982.

Müsch, A., Wiedmann, M., and Rapoport, T.A. (1992). Yeast Sec proteins interact with polypeptides traversing the endoplasmic reticulum membrane. Cell *69*, 343–352.

Nicchitta, C.V., Murphy, E.C.R., Haynes, R., and Shelness, G.S. (1995). Stage- and ribosome-specific alterations in nascent chain-Sec61p interactions accompany translocation across the ER membrane. J. Cell Biol. *129*, 957–970.

Ojakian, G.K., Kreibich, G., and Sabatini, D.D. (1977). Mobility of ribosomes bound to microsomal membranes. A freeze-etch and thin-section electron microscope study of the structure and fluidity of the rough endoplasmic reticulum. J. Cell Biol. *72*, 530–551.

Panzner, S., Dreier, L., Hartmann, E., Kostka, S., and Rapoport, T.A. (1995). Posttranslational protein transport in yeast reconstituted with a purified complex of Sec proteins and Kar2p. Cell *81*, 561–570.

Rapoport, T.A. (1985). Extensions of the signal hypothesis—sequential insertion model versus amphipathic tunnel hypothesis. FEBS Lett. *187*, 1–10.

Rapoport, T.A., Jungnickel, B., and Kutay, U. (1996). Protein transport across the eukaryotic endoplasmic reticulum and bacterial inner membranes. Annu. Rev. Biochem. *65*, 271–303.

Rothblatt, J.A., Deshaies, R.J., Sanders, S.L., Daum, G., and Schekman, R. (1989). Multiple genes are required for proper insertion of secretory proteins into the endoplasmic reticulum in yeast. J. Cell Biol. *109*, 2641–2652.

Sanders, S.L., Whitfield, K.M., Vogel, J.P., Rose, M.D., and Schekman, R.W. (1992). Sec61p and BiP directly facilitate polypeptide translocation into the ER. Cell *69*, 353–365.

Simon, S.M., and Blobel, G. (1991). A protein-conducting channel in the endoplasmic reticulum. Cell *65*, 371–380.

Singer, S., Maher, P., and Yaffe, M. (1987). On the transfer of integral proteins into membranes. Proc. Natl. Acad. Sci. USA *84*, 1960–1964.

Strambio-de-Castillia, C., Blobel, G., and Rout, M.P. (1995). Isolation and characterization of nuclear envelopes from the yeast Saccharomyces. J. Cell Biol. *131*, 19–31.

Wall, J.S., and Hainfeld, J.F. (1986). Mass mapping with the scanning transmission electron microscope. Annu. Rev. Biophys. Biophys. Chem. *15*, 355–376.

Walter, P., and Blobel, G. (1983). Preparation of microsomal membranes for cotranslational protein translocation. Meth. Enzymol. *96*, 84–93.

Walter, P., and Johnson, A.E. (1994). Signal sequence recognition and protein targeting to the endoplasmic reticulum membrane. Annu. Rev. Cell Biol. *10*, 87–119.

Walter, P., Ibrahimi, I., and Blobel, G. (1981). Translocation of proteins across the endoplasmic reticulum. I. Signal recognition protein (SRP) binds to in vitro assembled polysomes synthesizing secretory protein. J. Cell Biol. *91*, 545–550.